



ELSEVIER

Contents lists available at ScienceDirect

Meta Gene

journal homepage: www.elsevier.com/locate/mgene

Conserved secondary structures predicted within the 5' packaging signal region of influenza A virus PB2 segment

Yuki Kobayashi^{a,*,1}, Oliver G. Pybus^b, Takuya Itou^a, Yoshiyuki Suzuki^{c,1}

^a Nihon University Veterinary Research Center, Fujisawa, Kanagawa 252-0880, Japan

^b Department of Zoology, University of Oxford, Oxford OX1 3PS, United Kingdom

^c Graduate School of Natural Sciences, Nagoya City University, Nagoya, Aichi 467-8501, Japan

ARTICLE INFO

Keywords:

Influenza A virus
Secondary structure
Stem loop
Packaging signal
PB2 segment

ABSTRACT

Infectious particles of influenza A virus (IAV) typically contain eight unique negative-strand viral RNA (vRNA) segments. It has been suggested that the selective packaging of IAV segments occurs through RNA-RNA interactions between different vRNA segments, and that local secondary structures formed within vRNA segments are involved in such interactions. PB2 segment plays a critical role in the viral packaging process and 80–150 bases at the 5' end of PB2 vRNA sequence are thought to contain packaging signals. Here we show that the 5' packaging signal region of PB2 segment forms a stem-loop structure specifically in the negative-strand RNA in > 97% of 1703 IAV strains analyzed. This stem-loop structure is located at the nucleotide positions where synonymous mutations and partial deletions have been shown to markedly reduce the packaging efficiency of PB2 segment. These observations suggest that the stem-loop structure predicted in the present study is a component of packaging signal in PB2 segment.

1. Introduction

Influenza A virus (IAV), a member of the family *Orthomyxoviridae*, possesses a genome comprising eight segmented, negative-strand RNAs (vRNAs), which are essential for efficient virus replication. Each vRNA segment binds to polymerized nucleoproteins (NPs) and single molecules of the polymerase subunits PB2, PB1, and PA, thereby forming a viral ribonucleoprotein (vRNP) (Coloma et al., 2009; Arranz et al., 2012). Fully infectious IAV virions are thought to incorporate a single copy of each of the eight different vRNA segments, a process termed selective packaging (Hutchinson et al., 2010; Chou et al., 2012; Noda et al., 2012).

Experimental studies have shown that approximately 100 bases at each terminus of vRNA sequences, including the untranslated region (UTR) and a part of the coding region, are conserved among different IAV subtypes and are required for the selective packaging of vRNA segments into budding virions, suggesting that these terminal regions contain packaging signals responsible for selective packaging (Duhaut and Dimmock, 2000, 2002; Fujii et al., 2003, 2005; Dos Santos Afonso et al., 2005; Muramoto et al., 2006; Liang et al., 2005, 2008; Gog et al., 2007; Marsh et al., 2008; Ozawa et al., 2009). Although the mechanism by which packaging signals are coordinated and give rise to selective

packaging is not fully understood, it has been suggested that IAV selective packaging occurs through RNA-RNA interactions between different vRNA segments and that local secondary structures formed within vRNA segments are involved in such interactions (Fournier et al., 2012a, 2012b; Essere et al., 2013; Gavazzi et al., 2013).

Actually, it was previously considered that secondary structures that can be formed in vRNAs are melted by NP binding, and that NPs are uniformly distributed on vRNAs in vRNPs (Baudin et al., 1994). Recently, however, it has become evident that vRNAs form secondary structures in vRNPs. The studies using electron tomography revealed the existence of string-like structures between vRNPs in the IAV virions, which may represent vRNA regions released from NP binding (Fournier et al., 2012a, 2012b; Noda et al., 2012), and the high flexibility of vRNPs, which may allow the formation of secondary structures in vRNAs (Gallagher et al., 2017). The binding profile of NP on vRNAs identified by high-throughput sequencing of RNA isolated by cross-linking immunoprecipitation (HITS-CLIP) also showed many vRNA regions that were free from NP (Lee et al., 2017). We have discovered extremely conserved secondary structures involved in production of infectious virus particles in the packaging signal region of the M segment (Kobayashi et al., 2016). Local secondary structures containing pairs of co-varying nucleotide sites have also been found in the

* Corresponding author at: Nihon University Veterinary Research Center, 1866 Kameino, Fujisawa, Kanagawa 252-0880, Japan.

E-mail address: suzuki.yukikb@nihon-u.ac.jp (Y. Kobayashi).

¹ These authors contributed equally.

packaging signal regions of HA and NP segments (Gulyaev et al., 2014, 2016). Therefore, conserved secondary structures in vRNAs may be potential candidates for packaging signals in IAVs.

It has been observed that deletion of the PB2 vRNA segment had the strongest impact among eight segments on the packaging efficiencies of other vRNA segments (Muramoto et al., 2006; Gao et al., 2012), suggesting that the PB2 segment plays a critical role in the packaging process. Many experimental studies have shown that approximately 80–150 bases at the 5' end of PB2 vRNA sequence are needed for selective packaging, although the 3' end also demonstrated a moderate effect on the packaging of PB2 segment (Duhaut and Dimmock, 2000, 2002; Dos Santos Afonso et al., 2005; Muramoto et al., 2006; Liang et al., 2005, 2008; Gog et al., 2007; Marsh et al., 2008). In order to investigate whether the packaging signal region of PB2 vRNA forms secondary structures, we conducted *in-silico* prediction of secondary structures in the PB2 segment using 1703 sequences in this study. We found highly conserved secondary structures within the 5' packaging signal region specifically in the negative-strand PB2 sequence.

2. Results and discussion

2.1. Potential of forming local secondary structures in PB2 segment

Nucleotide sequences of PB2 segment for 1703 IAV strains belonging to 86 subtypes collected from human ($n = 409$), swine ($n = 146$), avian ($n = 1092$), and other host species ($n = 56$) were retrieved from the Influenza Virus Resource (Bao et al., 2008) and were analyzed in order to identify conserved secondary RNA structures (Table 1, Supplemental Table S1). The sliding window analysis was conducted for evaluating the potential of forming local secondary structures based on the z -score of minimum free energy (MFE) using the UNAFOLD program implemented in the SSE package (Markham and Zuker, 2008; Simmonds, 2012), where windows with negative z -scores were inferred to contain bases that form secondary structures.

The overall pattern of z -scores along the PB2 sequence was similar for both negative-sense RNA ($-$ RNA) and positive-sense RNA ($+$ RNA) (Fig. 1A). Interestingly, however, the window containing positions 2179–2328 showed a negative z -score (-0.8) in the $-$ RNA sequence but a positive z -score in the $+$ RNA sequence. It should be noted that packaging signals are thought to be located at these positions (Fig. 1C) (Duhaut and Dimmock, 2000, 2002; Dos Santos Afonso et al., 2005; Muramoto et al., 2006; Liang et al., 2005, 2008; Gog et al., 2007; Marsh et al., 2008). The bases at positions 2179–2328 were conserved among 1703 IAV strains with $> 95\%$ identities (Fig. 1C). In addition, synonymous substitution was suppressed at these positions; the d_s values for the windows at these positions fell within the lowest 5% of the d_s values for all windows (Fig. 1B). In particular, the d_s value at positions 2269–2283 was 0.00014, which was the lowest among all the windows analyzed. These results suggest the presence of functional RNA secondary structures at the 5' packaging signal region of PB2 $-$ RNA.

Table 1

Hosts and subtypes of PB2 sequences used in the present study.

Segment	Host	Subtype
PB2 (1703)	Human(409), Swine(146), Avian(1092), Equine(2), Ferret(1), Pika(1), Seal(2), Environment(44), Stone marten(1), Unknown(5)	H1N1(308), H1N2(42), H1N3(3), H1N5(1), H1N6(2), H1N9(2), H2N1(2), H2N2(8), H2N3(19), H2N4(1), H2N5(2), H2N7(2), H2N8(2), H2N9(2), H3N1(8), H3N2(221), H3N3(5), H3N6(22), H3N7(1), H3N8(110), H3N9(2), H4N1(1), H4N2(8), H4N3(2), H4N5(1), H4N6(75), H4N7(1), H4N8(18), H4N9(2), H5N1(119), H5N2(128), H5N3(15), H5N4(3), H5N5(3), H5N6(1), H5N7(5), H5N8(2), H5N9(2), H6N1(80), H6N2(26), H6N3(4), H6N4(1), H6N5(10), H6N6(6), H6N8(6), H6N9(1), H7N1(6), H7N2(9), H7N3(29), H7N5(2), H7N6(2), H7N7(15), H7N9(2), H8N3(1), H8N4(17), H9N1(8), H9N2(95), H9N5(5), H9N6(2), H9N7(2), H9N9(3), H10N1(1), H10N2(1), H10N3(8), H10N6(2), H10N7(45), H10N8(3), H10N9(2), H11N1(1), H11N2(8), H11N3(3), H11N5(1), H11N6(3), H11N9(30), H12N3(1), H12N4(1), H12N5(13), H12N6(2), H12N8(1), H12N9(1), H13N2(1), H13N6(2), H13N9(1), H15N9(1), H16N3(1)

The numbers in parentheses indicate the total number of isolates. The accession numbers for sequences are shown in Supplemental Table S1.

2.2. Prediction of local secondary structures in PB2 segment

Secondary structures that may be formed at positions 2179–2328 of PB2 $-$ RNA segment were predicted with RNAalifold (Bernhart et al., 2008). Analyses were undertaken using three datasets of partial PB2 nucleotide sequences of positions 2179–2328, each of which was obtained by randomly choosing 10 sequences from 1703 PB2 $-$ RNA sequences (Supplemental Table S2). The stem-loop (SL) structure consisting of three stems and three internal loops was predicted at positions 2256–2308 in all datasets (Supplemental Fig. S1). The same SL structure was also predicted when the complete $-$ RNA PB2 nucleotide sequence was used for prediction (Supplemental Fig. S2). In contrast, the SL structure was not predicted at the corresponding positions in the PB2 $+$ RNA sequences (data not shown), supporting the above result showing a positive MFE z -score at these positions in the PB2 $+$ RNA sequence (Fig. 1A).

When the secondary structure was predicted at positions 2179–2328 for each of 1703 PB2 $-$ RNA sequences using RNAfold (Zuker, 2003), $> 97\%$ of the sequences were found to form either one of two SL structures, SL-I or SL-II, which had different internal loop structures at positions 2271–2293 (Fig. 2A, B) but shared a stable stem formed between positions 2256–2270 and 2294–2308 (Fig. 2C). Thus most IAVs appear to form SL structures within the 5' packaging signal region of PB2 vRNA. The MFE to form the SL structures ranged from -9.8 to -20.4 kcal/mol. The bases with the lowest d_s value mainly constituted loops in the SL structure (Fig. 2A, B), which may be able to interact with other vRNAs.

2.3. Mapping nucleotide positions where mutations reduced packaging efficiency of PB2 segment

The functional relevance of the SL structure predicted above was assessed using the results obtained from previous experimental studies. Giannecchini et al. (2009, 2011) showed that synthetic phosphorothioate oligonucleotides (S-ONs) derived from the complementary nucleotide sequence of positions 2282–2291 (designated S-ON 5-15b), which was located within the SL structure (Fig. 3), markedly inhibited the replication of IAV and influenza B virus (IBV), while other S-ONs derived from surrounding complementary nucleotide sequences did not affect virus replication. The effect of S-ON 5-15b on IAV/IBV replication suggests that the target nucleotide sites of S-ON 5-15b are accessible in vRNA (Lenartowicz et al., 2016). Muramoto et al. (2006) additionally showed that 30 bases at the 5' coding region, including the target sites of S-ON 5-15b, were critical for packaging of PB2 segment.

Synonymous mutations and partial deletions have also been introduced to the PB2 vRNA sequence for examining their effects on the packaging efficiency of PB2 segment or a PB2-analog encoding GFP protein (Muramoto et al., 2006; Gog et al., 2007; Marsh et al., 2008; Liang et al., 2008). The nucleotide positions of the synonymous mutations (Gog et al., 2007; Marsh et al., 2008) and the partial deletions

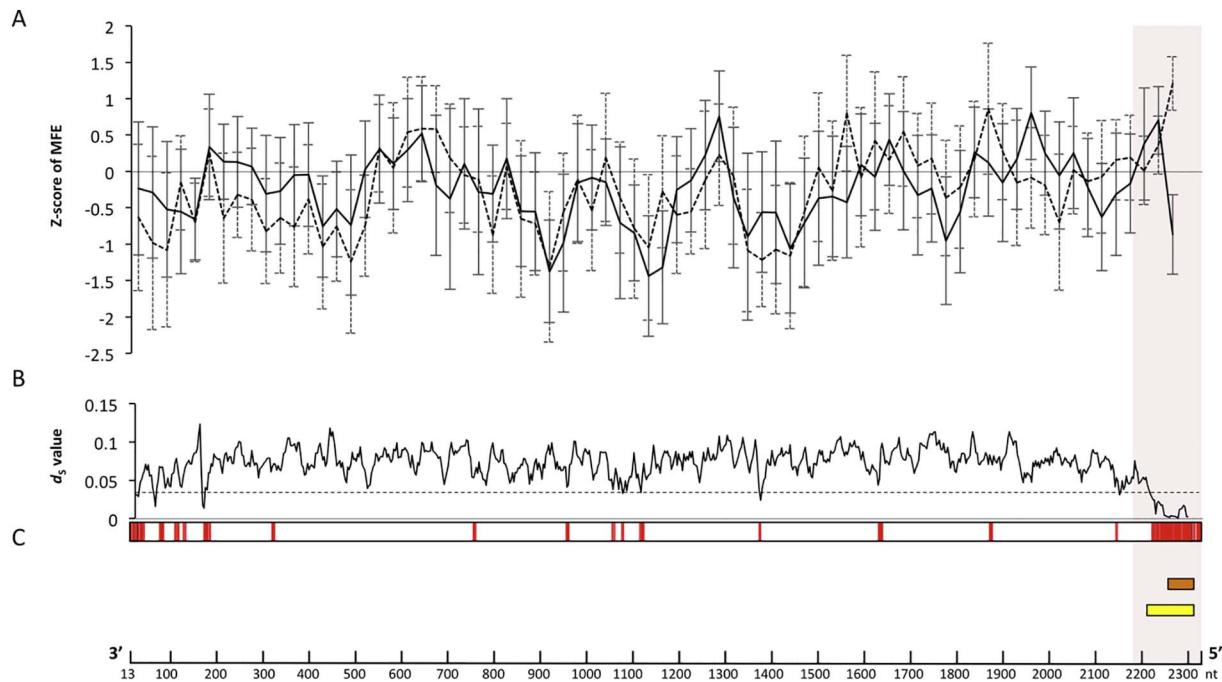


Fig. 1. Conserved secondary structures among 1703 PB2 segment vRNA sequences.

(A) The z -score of the minimum free energy for the secondary structures potentially formed by the nucleotide sequences in each window, calculated using SSE (Simmonds, 2012). 1703 PB2 sequences at nucleotide positions 13–2329 were used for the calculation of the z -score. The z -score at a window was calculated by randomizing the nucleotide sequences in the window 100 times using the dinucleotide model. Windows with negative z -scores were inferred to contain bases that form secondary structures. The window size was set at 150 bases and the step size at 30 bases. The z -score with standard deviation was represented by solid and broken lines for $-$ RNA and $+$ RNA, respectively. The pink shaded area highlights positions 2179–2328, which exhibited negative z -scores only in the $-$ RNA sequence. (B) The d_s values in the coding region, calculated using ADAPTSITE (Suzuki et al., 2001). The window was 5 codons wide and was moved in steps of 1 codon. The broken line represents the threshold ($d_s = 0.03$) for the lowest 5% of the d_s value among all windows. (C) Nucleotide sites with high identity. Stretches of > 6 nucleotide sites in which each nucleotide site exhibited $> 95\%$ identity are colored red. The orange box shows the location of the SL structure predicted at positions 2256–2308. The yellow box represents the nucleotide sites where the packaging signal is thought to be located (Duhaut and Dimmock, 2000, 2002; Dos Santos Afonso et al., 2005; Muramoto et al., 2006; Liang et al., 2005, 2008; Gog et al., 2007; Marsh et al., 2008). Nucleotide positions refer to those of the $+$ RNA sequence of the PB2 segment for A/hvPR8/34(H1N1) (accession number EF190971). (For interpretation of the references to color in this figure legend, the reader is referred to the web version of this article.)

(Muramoto et al., 2006; Liang et al., 2008) were mapped on the nucleotide sequence of the A/WSN/33(H1N1) strain (accession number CY010795) (Fig. 3). These positions were evenly distributed in both the stem and internal-loop regions of the SL structure. However, synonymous mutations at positions 2220 (mut731) and 2238 (mut737), which were mapped outside the SL structure, had less impact on the packaging efficiency of PB2 segment than mutations mut744a, mut744b, mut745, mut748, mut751, and mut757, which were mapped inside the SL structure. Similarly, influence of multiple-synonymous mutations introduced outside the SL structure at positions 2211–2250 (PB2-51 and PB2-52) on the packaging efficiency of PB2 segment was smaller than those introduced inside the SL structure (PB2-53, PB2-54, and PB2-56). The probability of observing that all sets of synonymous mutations introduced in the SL structure (mut744a, mut744b, mut745, mut748, mut751, mut757, PB2-53, PB2-54, and PB2-52) had a stronger impact on the packaging efficiency of PB2 segment than all sets of synonymous mutations introduced in the surrounding region (mut731, mut737, PB2-51, and PB2-52) by chance is 0.0014, indicating that the SL structure is associated with the packaging efficiency of PB2 segment. These observations suggest that the SL structure predicted in the present study is a component of packaging signal in PB2 segment.

2.4. Secondary structure formation within packaging signal region of vRNAs in vRNPs

Recently, it was reported using HITS-CLIP that the 5' and 3' terminal regions of vRNAs in many vRNPs were bound by NPs (Lee et al., 2017), which may melt the secondary structures that can be formed in vRNAs (Baudin et al., 1994). These regions were also found to be inaccessible by antisense oligonucleotides, suggesting the absence of secondary

structures at these regions including the 5' packaging signal region of PB2 vRNA (Lee et al., 2017). These observations are in sharp contrast to the previous findings in many studies that the 5' and 3' terminal regions of each vRNA sequence contain packaging signals, which apparently exert their functions through direct RNA-RNA interactions upon formation of local secondary structures (Gog et al., 2007; Liang et al., 2008; Marsh et al., 2008; Fournier et al., 2012a, 2012b; Essere et al., 2013; Gavazzi et al., 2013). In particular, functional secondary structures have been identified in the packaging signal regions of HA, NP (Gulyaev et al., 2014, 2016), and M segments (Kobayashi et al., 2016). In addition, inhibition of IAV/IBV replication by S-ON 5-15b as mentioned above indicates that the target nucleotide sites of S-ON 5-15b in the 5' packaging signal region of PB2 vRNA form loop structures (Giannecchini et al., 2009), as predicted in the present study. It should be noted that, in the HITS-CLIP analysis, the NP-binding regions of vRNAs were identified by sequencing the RNA segments that remained bound to NP after digestion with RNase A, which specifically cleaves single-stranded RNAs (Lee et al., 2017). Therefore, the results may be affected if vRNAs form secondary structures including double-stranded RNAs in vRNPs. Taken together, these observations suggest that the secondary structure predicted in the present study is a genuine component of packaging signal in PB2 segment.

Supplementary data to this article can be found online at <https://doi.org/10.1016/j.mgene.2017.11.006>.

Acknowledgements

This work was supported by a Japan Society for the Promotion of Science grant to YK (24-448), by a Grant-in-Aid for Scientific Research on Innovative Areas from the Ministry of Education, Culture, Sports,

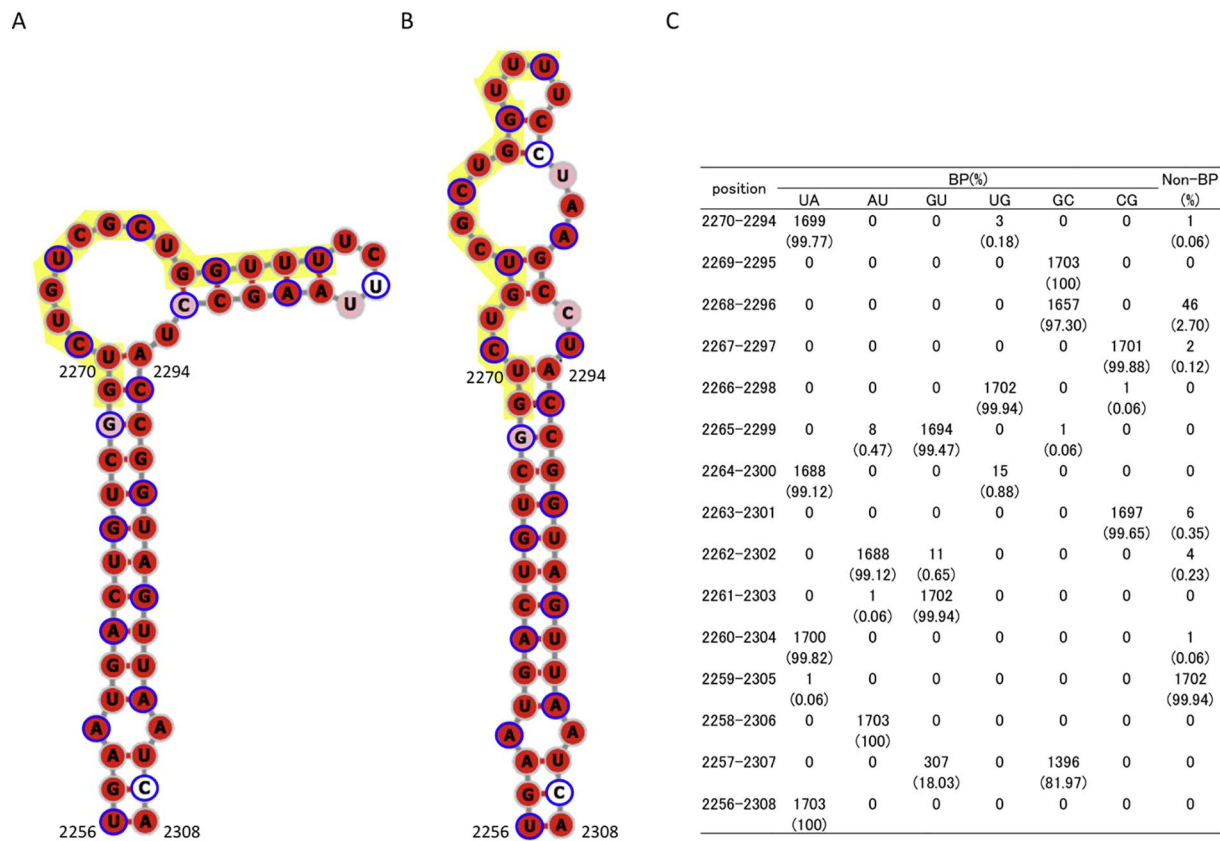


Fig. 2. SL-I and SL-II structures predicted in -RNA PB2 segment sequences. The background red, pink, and white colors of each base represents identities of > 98%, 90–98%, and < 90% among 1703 PB2 sequences, respectively. Third codon positions are circled blue. Yellow-filled boxes represent the codon positions with the d_s values of < 0.00014. Nucleotide positions are numbered according to the PB2 + RNA sequence of A/hvPR8/34(H1N1) (accession number EF190971). (A) SL-I structure predicted in the PB2 sequence of A/WSN/1933(H1N1) (accession number CY010795). (B) SL-II structure predicted in the PB2 sequence of A/northern shoveler/Missouri/196/2009(H10N3) (accession number CY097621). (C) The number of sequences that were predicted to form base-pairing (BP) at the stem of SL-I and SL-II among 1703 sequences. (For interpretation of the references to color in this figure legend, the reader is referred to the web version of this article.)

Science and Technology (MEXT) of Japan (No. 17H05824) to YK, and by the Strategic Research Base Development Program, “International joint research and training of young researchers for zoonosis control in a globalized world”, and a matching fund subsidy from the Ministry of

Education, Culture, Sports, Science and Technology (MEXT) of Japan to YK and TI (S1491007).

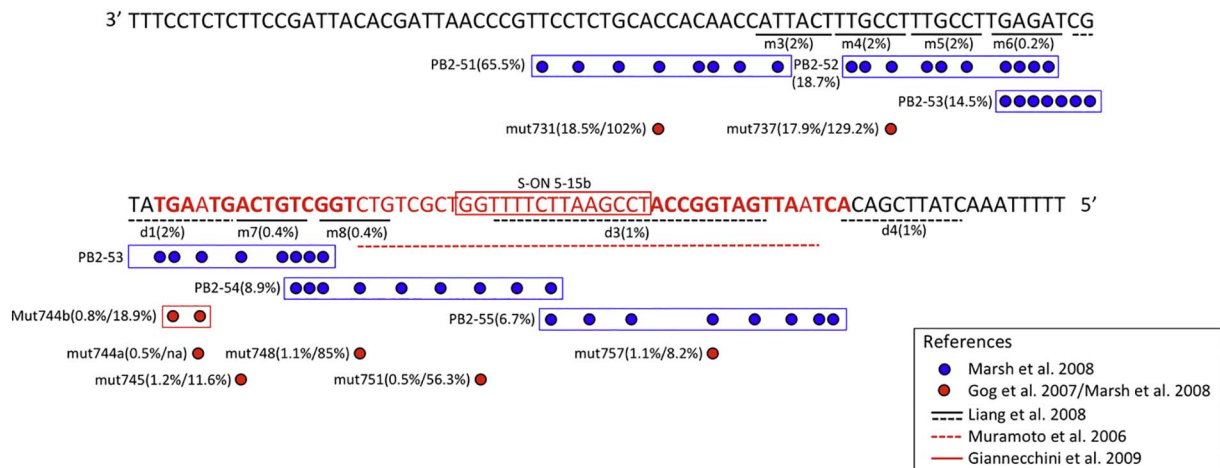


Fig. 3. Nucleotide positions where synonymous mutations and partial deletions reduced packaging efficiency of PB2 segment. Nucleotide sequence at positions 2179–2315 of WSN strain (accession number CY010795). Red bases are inferred to form the SL-I structure (bold-face: stem; plain-text: loop). Filled circles and black solid lines below the bases denote the positions where synonymous mutations were introduced to investigate the packaging efficiency of PB2 segment (Gog et al., 2007; Liang et al., 2008; Marsh et al., 2008), and black broken lines below the bases denote the deleted positions (Liang et al., 2008). Percentages in parentheses show the relative PB2 packaging efficiency when synonymous mutations or partial deletions were introduced to the corresponding positions (Gog et al., 2007; Marsh et al., 2008; Liang et al., 2008). Bases in the red box are the target sites of S-ON 5-15b (Giannecchini et al., 2009). The red broken line below the bases denotes the critical positions of PB2 packaging reported by Muramoto et al. (2006). (For interpretation of the references to color in this figure legend, the reader is referred to the web version of this article.)

Author contributions

YK, OP, and YS designed the study, and YK carried out the analyses. All authors contributed to the writing of the manuscript.

Conflicts of interest

The authors declare no conflict of interest.

References

- Arranz, R., Coloma, R., Chichón, F.J., Conesa, J.J., Carrascosa, J.L., Valpuesta, J.M., Ortín, J., Martín-Benito, J., 2012. The structure of native influenza virion ribonucleoproteins. *Science* 338, 1634–1637.
- Bao, Y., Bolotov, P., Dernovoy, D., Kiryutin, B., Zaslavsky, L., Tatusova, T., Ostell, J., Lipman, D., 2008. The influenza virus resource at the National Center for Biotechnology Information. *J. Virol.* 82, 596–601.
- Baudin, F., Bach, C., Cusack, S., Ruigrok, R.W., 1994. Structure of influenza virus RNP. I. Influenza virus nucleoprotein melts secondary structure in panhandle RNA and exposes the bases to the solvent. *EMBO J.* 13, 3158–3165.
- Bernhart, S.H., Hofacker, I.L., Will, S., Gruber, A.R., Stadler, P.F., 2008. RNAalifold: improved consensus structure prediction for RNA alignments. *BMC Bioinf.* 9, 474.
- Chou, Y.Y., Vafabakhsh, R., Doğanay, S., Gao, Q., Ha, T., Palese, P., 2012. One influenza virus particle packages eight unique viral RNAs as shown by FISH analysis. *Proc. Natl. Acad. Sci. U. S. A.* 109, 9101–9106.
- Coloma, R., Valpuesta, J.M., Arranz, R., Carrascosa, J.L., Ortín, J., Martín-Benito, J., 2009. The structure of a biologically active influenza virus ribonucleoprotein complex. *PLoS Pathog.* 5, e1000491.
- Dos Santos Afonso, E., Escriu, N., Leclercq, I., van der Werf, S., Naffakh, N., 2005. The generation of recombinant influenza A viruses expressing a PB2 fusion protein requires the conservation of a packaging signal overlapping the coding and noncoding regions at the 5′ end of the PB2 segment. *Virology* 341, 34–46.
- Duhaut, S.D., Dimmock, N.J., 2000. Approximately 150 nucleotides from the 5′ end of an influenza A segment 1 defective virion RNA are needed for genome stability during passage of defective virus in infected cells. *Virology* 275, 278–285.
- Duhaut, S.D., Dimmock, N.J., 2002. Defective segment 1 RNAs that interfere with production of infectious influenza A virus require at least 150 nucleotides of 5′ sequence: evidence from a plasmid-driven system. *J. Gen. Virol.* 83, 403–411.
- Essere, B., Yver, M., Gavazzi, C., Terrier, O., Isel, C., Fournier, E., Giroux, F., Textoris, J., Julien, T., Socratous, C., Rosa-Calatrava, M., Lina, B., Marquet, R., Moules, V., 2013. Critical role of segment-specific packaging signals in genetic reassortment of influenza A viruses. *Proc. Natl. Acad. Sci. U. S. A.* 110, E3840–3848.
- Fournier, E., Moules, V., Essere, B., Paillart, J.C., Sirbat, J.D., Isel, C., Cavalier, A., Rolland, J.P., Thomas, D., Lina, B., et al., 2012a. A supramolecular assembly formed by influenza A virus genomic RNA segments. *Nucleic Acids Res.* 40, 2197–2209.
- Fournier, E., Moules, V., Essere, B., Paillart, J.C., Sirbat, J.D., Cavalier, A., Rolland, J.P., Thomas, D., Lina, B., Isel, C., Marquet, R., 2012b. Interaction network linking the human H3N2 influenza A virus genomic RNA segments. *Vaccine* 30, 7359–7367.
- Fujii, Y., Goto, H., Watanabe, T., Yoshida, T., Kawaoka, Y., 2003. Selective incorporation of influenza virus RNA segments into virions. *Proc. Natl. Acad. Sci. U. S. A.* 100, 2002–2007.
- Fujii, K., Fujii, Y., Noda, T., Muramoto, Y., Watanabe, T., Takada, A., Goto, H., Horimoto, T., Kawaoka, Y., 2005. Importance of both the coding and the segment-specific noncoding regions of the influenza A virus NS segment for its efficient incorporation into virions. *J. Virol.* 79, 3766–3774.
- Gallagher, J.R., Torian, U., McCraw, D.M., Harris, A.K., 2017. Structural studies of influenza virus RNPs by electron microscopy indicate molecular contortions within NP supra-structures. *J. Struct. Biol.* 197, 294–307.
- Gao, Q., Chou, Y.Y., Doğanay, S., Vafabakhsh, R., Ha, T., Palese, P., 2012. The influenza A virus PB2, PA, NP, and M segments play a pivotal role during genome packaging. *J. Virol.* 86, 7043–7051.
- Gavazzi, C., Yver, M., Isel, C., Smyth, R.P., Rosa-Calatrava, M., Lina, B., Moulès, V., Marquet, R., 2013. A functional sequence-specific interaction between influenza A virus genomic RNA segments. *Proc. Natl. Acad. Sci. U. S. A.* 110, 16604–16609.
- Giannecchini, S., Clausi, V., Nosi, D., Azzi, A., 2009. Oligonucleotides derived from the packaging signal at the 5′ end of the viral PB2 segment specifically inhibit influenza virus in vitro. *Arch. Virol.* 154, 821–832.
- Giannecchini, S., Wise, H.M., Digard, P., Clausi, V., Del Poggetto, E., Vesco, L., Puzelli, S., Donatelli, I., Azzi, A., 2011. Packaging signals in the 5′-ends of influenza virus PA, PB1, and PB2 genes as potential targets to develop nucleic-acid based antiviral molecules. *Antivir. Res.* 92, 64–72.
- Gog, J.R., Afonso Edos, S., Dalton, R.M., Leclercq, I., Tiley, L., Elton, D., von Kirchbach, J.C., Naffakh, N., Escriu, N., Digard, P., 2007. Codon conservation in the influenza A virus genome defines RNA packaging signals. *Nucleic Acids Res.* 35, 1897–1907.
- Gulyaev, A.P., Tsyganov-Bodounov, A., Spronken, M.I., van der Kooij, S., Fouchier, R.A., Olsthoorn, R.C., 2014. RNA structural constraints in the evolution of the influenza A virus genome NP segment. *RNA Biol.* 11, 942–952.
- Gulyaev, A.P., Spronken, M.I., Richard, M., Schrauwen, E.J., Olsthoorn, R.C., Fouchier, R.A., 2016. Subtype-specific structural constraints in the evolution of influenza A virus hemagglutinin genes. *Sci. Rep.* 6, 38892.
- Hutchinson, E.C., von Kirchbach, J.C., Gog, J.R., Digard, P., 2010. Genome packaging in influenza A virus. *J. Gen. Virol.* 91, 313–328.
- Kobayashi, Y., Dadonaite, B., van Doremalen, N., Suzuki, Y., Barclay, W.S., Pybus, O.G., 2016. Computational and molecular analysis of conserved influenza A virus RNA secondary structures involved in infectious virion production. *RNA Biol.* 13, 883–894.
- Lee, N., Le Sage, V., Nanni, A.V., Snyder, D.J., Cooper, V.S., Lakdawala, S.S., 2017. Genome-wide analysis of influenza viral RNA and nucleoprotein association. *Nucleic Acids Res.* 45, 8968–8977.
- Lenartowicz, E., Nogales, A., Kierzek, E., Kierzek, R., Martínez-Sobrido, L., Turner, D.H., 2016. Antisense oligonucleotides targeting influenza A segment 8 genomic RNA inhibit viral replication. *Nucleic Acid Ther.* 26, 277–285.
- Liang, Y., Hong, Y., Parslow, T.G., 2005. cis-Acting packaging signals in the influenza virus PB1, PB2, and PA genomic RNA segments. *J. Virol.* 79, 10348–10355.
- Liang, Y., Huang, T., Ly, H., Parslow, T.G., Liang, Y., 2008. Mutational analyses of packaging signals in influenza virus PA, PB1, and PB2 genomic RNA segments. *J. Virol.* 82, 229–236.
- Markham, N.R., Zuker, M., 2008. UNAFold: software for nucleic acid folding and hybridization. *Methods Mol. Biol.* 453, 3–31.
- Marsh, G.A., Rabadán, R., Levine, A.J., Palese, P., 2008. Highly conserved regions of influenza A virus polymerase gene segments are critical for efficient viral RNA packaging. *J. Virol.* 82, 2295–2304.
- Muramoto, Y., Takada, A., Fujii, K., Noda, T., Iwatsuki-Horimoto, K., Watanabe, S., Horimoto, T., Kida, H., Kawaoka, Y., 2006. Hierarchy among viral RNA (vRNA) segments in their role in vRNA incorporation into influenza A virions. *J. Virol.* 80, 2318–2325.
- Noda, T., Sugita, Y., Aoyama, K., Hirase, A., Kawakami, E., Miyazawa, A., Sagara, H., Kawaoka, Y., 2012. Three-dimensional analysis of ribonucleoprotein complexes in influenza A virus. *Nat. Commun.* 3, 639.
- Ozawa, M., Maeda, J., Iwatsuki-Horimoto, K., Watanabe, S., Goto, H., Horimoto, T., Kawaoka, Y., 2009. Nucleotide sequence requirements at the 5′ end of the influenza A virus M RNA segment for efficient virus replication. *J. Virol.* 83, 3384–3388.
- Simmonds, P., 2012. SSE: a nucleotide and amino acid sequence analysis platform. *BMC Res. Notes* 5, 50.
- Suzuki, Y., Gojobori, T., Nei, M., 2001. ADAPTSITE: detecting natural selection at single amino acid sites. *Bioinformatics* 17, 660–661.
- Zuker, M., 2003. Mfold web server for nucleic acid folding and hybridization prediction. *Nucleic Acids Res.* 31, 3406–3415.